

JOM 23387

# Crystal structure of $[\text{CF}_3\text{CF}=\text{C}(\text{CF}_3)\text{Ag}]_4$ and its use as a chemical vapor deposition precursor for silver films

Patrick M. Jeffries, Scott R. Wilson and Gregory S. Girolami

School of Chemical Sciences and Materials Research Laboratory, University of Illinois at Urbana-Champaign, 505 South Mathews Avenue, Urbana, IL 61801 (USA)

(Received August 12th, 1992)

## Abstract

Silver films have been prepared by the metal-organic chemical vapor deposition of perfluoro-1-methyl-1-propenylsilver tetramer,  $[\text{CF}_3\text{CF}=\text{C}(\text{CF}_3)\text{Ag}]_4$ , at 275°C and  $10^{-4}$  Torr; the silver films contain only traces (<1%) of fluorine and oxygen and no carbon. The principal organic byproducts formed during deposition are *trans*- $\text{CF}_3\text{CF}=\text{CH}(\text{CF}_3)$  (50%) and  $\text{CF}_3\text{C}\equiv\text{CCF}_3$  (40%). It is argued that silver metal is produced by elimination of  $\text{CF}_3\text{C}\equiv\text{CCF}_3$  from *trans*- $[\text{CF}_3\text{CF}=\text{C}(\text{CF}_3)\text{Ag}]_4$  to form silver(I) fluoride, which defluorinates to form silver metal. The crystal structure of *trans*- $[\text{CF}_3\text{CF}=\text{C}(\text{CF}_3)\text{Ag}]_4$  was determined and reveals that this compound is a tetramer that consists of a square plane of silver atoms in which each edge is bridged by a *trans*-perfluoro-1-methyl-1-propenyl ligand. The average distances and angles are: Ag–Ag = 2.761 Å, Ag–C = 2.19 Å, Ag–C–Ag = 78.3° and C–Ag–C = 166.7°. Crystal data: monoclinic, space group  $P2_1/c$ ,  $a = 9.480(5)$  Å,  $b = 15.589(6)$  Å,  $c = 18.919(4)$  Å,  $\beta = 90.27(3)^\circ$ ,  $V = 2796(4)$  Å<sup>3</sup>,  $Z = 4$ ,  $R_F = 0.070$ , and  $R_{wF} = 0.089$  on 433 variables and 3617 data with  $I > 2.58 \sigma(I)$ .

## 1. Introduction

Silver has been shown to be an attractive dopant in high- $T_c$  superconductors because it promotes crystallization and c-axis orientation, strengthens intergranular coupling, improves surface smoothness, and increases  $T_c$  and  $J_c$  [1–7]. Although many high- $T_c$  superconducting phases have been deposited by thermal metal-organic chemical vapor deposition (MOCVD) routes [8–11], no silver-containing high- $T_c$  superconducting phases have been deposited by a thermal MOCVD process. Accordingly, we have initiated an investigation to evaluate the potential of volatile silver complexes to serve as MOCVD precursors to silver-containing thin films.

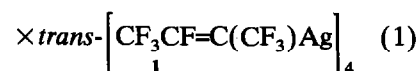
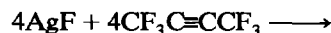
Since  $\sigma$ -bonded organosilver complexes are known to decompose in solution to yield silver metal [12], such compounds are attractive candidates as possible MOCVD precursors. In fact, Suhr [13] has shown that pure silver films can be obtained by plasma-enhanced chemical vapor deposition from the *trans*-perfluoro-1-methyl-1-propenylsilver tetramer,  $[\text{CF}_3\text{CF}=\text{C}(\text{CF}_3)\text{Ag}]_4$

(1). We have now undertaken studies in order to determine whether this precursor can also deposit silver films under thermal MOCVD conditions. We also describe the crystal structure of  $[\text{CF}_3\text{CF}=\text{C}(\text{CF}_3)\text{Ag}]_4$  and investigations of the mechanism by which this precursor yields silver deposits.

## 2. Results and discussion

### 2.1. Crystallographic studies

*trans*-Perfluoro-1-methyl-1-propenylsilver tetramer,  $[\text{CF}_3\text{CF}=\text{C}(\text{CF}_3)\text{Ag}]_4$  (1) is prepared by the addition of  $\text{CF}_3\text{C}\equiv\text{CCF}_3$  to AgF in acetonitrile and is purified by sublimation [14]. If desired, 1 may be further purified by recrystallization from methylene chloride.



Because  $\sigma$ -bonded organosilver complexes are usually temperature, light, and moisture sensitive, little structural information is available and in particular, no alkenylsilver complexes have been crystallographically characterized [12,15]. Therefore, we have carried out an X-ray crystallographic study of 1. Crystal data are

Correspondence to: Professor G.S. Girolami.

presented in Table 1, atomic coordinates are shown in Table 2, and selected bond distances and angles are given in Table 3.

Crystals of **1**, grown from  $\text{CH}_2\text{Cl}_2$ , are monoclinic, and there is one molecule in the asymmetric unit; molecules of **1** lie on general positions within the unit cell (Figs. 1 and 2). The compound has a tetrameric structure that consists of a square plane of silver atoms in which each edge is bridged by a *trans*-perfluoro-1-methyl-1-propenyl ligand. The tetrameric structure is consistent with previous mass spectrometric studies, which revealed that the compound was at least a tetramer in the gas phase [13], and the presence of *trans*-perfluoroalkenyl ligands (as opposed to the *cis* isomer) is consistent with previous solution NMR studies [14].

The structure of **1** is best compared with those of the only other tetrameric organosilver compounds,  $[\text{CpFe}(\text{C}_5\text{H}_3\text{CH}_2\text{NMe}_2)\text{Ag}]_4$  (**2**) [16] and  $[\text{Me}_3\text{C}_6\text{H}_2\text{Ag}]_4$  (**3**) [17]. In all three compounds **1**–**3**, the silver atoms are two coordinate and assume nearly linear geometries; furthermore, in each case the silver atom is interacting with an  $\text{sp}^2$  carbon atom. Given these similarities, it is not surprising that the average bond distances and angles in **1**–**3** are very similar: the average Ag–Ag distance is 2.761 Å in **1**, 2.740 Å in **2**, and 2.744 Å in **3**; the average Ag–C distance is 2.19 Å in **1**, 2.17 Å in **2**, and 2.20 Å in **3**; the average C–Ag–C angle is 166.7° in **1**, 170.7° in **2**, and 167.1° in **3**; and the average Ag–C–Ag angle is 78.3° in **1**, 78.3° in **2**, and 77.05° in **3**. The Ag–C distance in **1** can also be compared with that of 2.19(2) and 2.10(1) Å in the mononuclear silver perfluoroalkyl complexes  $[(\text{CF}_3)_2\text{CF}]_2\text{Ag}^-$  and  $(\text{CF}_3)_2\text{CFAg}(\text{CH}_3\text{CN})$  [18].

TABLE 1. Crystallographic data for  $[\text{CF}_3\text{CF}=\text{C}(\text{CF}_3)\text{Ag}]_4$  (**1**) at  $-75^\circ\text{C}$

Space group: $P2_1/c$	$V = 2796$ (4) Å <sup>3</sup>
$a = 9.480$ (5) Å	$Z = 4$
$b = 15.589$ (6) Å	mol wt = 1155.60
$c = 18.919$ (4) Å	$d_{\text{calcd}} = 2.745$ g cm <sup>-3</sup>
$\beta = 90.27$ (3)°	$\mu_{\text{calcd}} = 29.29$ cm <sup>-1</sup>
$\alpha = \gamma = 90^\circ$	size = $0.3 \times 0.4 \times 0.4$ mm
diffractometer: Enraf-Nonius CAD4	
radiation: Mo K $\alpha$ , $\lambda = 0.71073$ Å	
monochromator: graphite crystal, $2\theta = 12^\circ$	
scan range, type: $2.0 < 2\theta < 58.0^\circ$ , $\omega/\theta$	
scan speed, width: $3\text{--}16^\circ \text{min}^{-1}$ , $\Delta\omega = 1.50[1.00 + 0.35 \tan \theta]^\circ$	
rflctns: 8276, 7401 unique, 3617 with $I > 2.58\sigma(I)$	
internal consistency: $R_1 = 0.019$	
$R_F = 0.070$	variables = 433
$R_{wF} = 0.089$	$p$ factor = 0.02

TABLE 2. Atomic Coordinates for  $[\text{CF}_3\text{CF}=\text{C}(\text{CF}_3)\text{Ag}]_4$  (**1**)

	x	y	z
Ag1	0.7545(1)	0.21894(9)	0.79613(5)
Ag2	0.4967(1)	0.2189(1)	0.86226(5)
Ag3	0.6273(1)	0.2571(1)	0.98880(5)
Ag4	0.8868(1)	0.25773(9)	0.92349(5)
F1	0.475(1)	0.0668(10)	0.6846(7)
F2	0.565(1)	0.245(1)	0.6401(6)
F3	0.359(1)	0.230(1)	0.6785(7)
F4	0.499(2)	0.3166(10)	0.7209(9)
F5	0.655(2)	0.0521(9)	0.8471(8)
F6	0.476(1)	−0.0143(9)	0.8161(8)
F7	0.667(2)	−0.0228(10)	0.7548(9)
F8	0.191(1)	0.2575(9)	1.0107(7)
F9	0.344(1)	0.4132(7)	1.0126(6)
F10	0.238(1)	0.3853(9)	0.9174(9)
F11	0.461(2)	0.411(1)	0.9169(8)
F12	0.456(2)	0.0948(8)	0.9859(9)
F13	0.328(1)	0.1228(9)	1.0701(5)
F14	0.236(1)	0.0959(9)	0.9699(6)
F15	0.930(1)	0.2187(8)	1.1405(4)
F16	1.0033(10)	0.3800(7)	1.0766(6)
F17	0.804(1)	0.3820(9)	1.1279(6)
F18	0.820(2)	0.4179(8)	1.0239(8)
F19	0.979(1)	0.0774(8)	1.0681(7)
F20	0.760(1)	0.0832(7)	1.1009(5)
F21	0.816(1)	0.0954(7)	0.9925(5)
F22	1.1348(10)	0.3365(8)	0.7571(5)
F23	1.0889(9)	0.1554(7)	0.7371(4)
F24	1.028(1)	0.1080(7)	0.8344(6)
F25	1.2026(8)	0.1888(7)	0.8302(5)
F26	0.810(2)	0.405(1)	0.830(1)
F27	1.010(2)	0.4655(9)	0.8314(9)
F28	0.903(2)	0.4385(8)	0.7364(6)
C1	0.551(1)	0.1813(10)	0.7544(7)
C2	0.537(2)	0.099(1)	0.7413(7)
C3	0.492(1)	0.237(1)	0.6974(6)
C4	0.583(1)	0.0296(10)	0.7905(9)
C5	0.405(2)	0.281(1)	0.9604(8)
C6	0.316(1)	0.228(1)	0.9896(8)
C7	0.357(1)	0.373(1)	0.9522(7)
C8	0.341(1)	0.1345(10)	1.0017(6)
C9	0.836(1)	0.2731(9)	1.0352(8)
C10	0.875(2)	0.2082(9)	1.0759(6)
C11	0.867(1)	0.3591(9)	1.0686(6)
C12	0.856(1)	0.1152(8)	1.0570(6)
C13	0.972(1)	0.2509(8)	0.8181(7)
C14	1.017(1)	0.3252(9)	0.7934(7)
C15	1.0737(10)	0.1788(8)	0.8037(5)
C16	0.934(2)	0.4067(8)	0.7991(8)

The Ag–Ag distances in **1**–**3** are short enough to suggest that there may be weak bonding interactions between the silver atoms; for comparison, the Ag–Ag distance in silver metal is 2.89 Å [19]. Although the silver centers have  $d^{10}$  electronic configurations, mixing between the filled  $d_{z^2}$  and empty  $p_z$  orbitals on silver can lead to a net bonding interaction, as has been discussed for other  $d^{10}$  species [20]. It is also worth

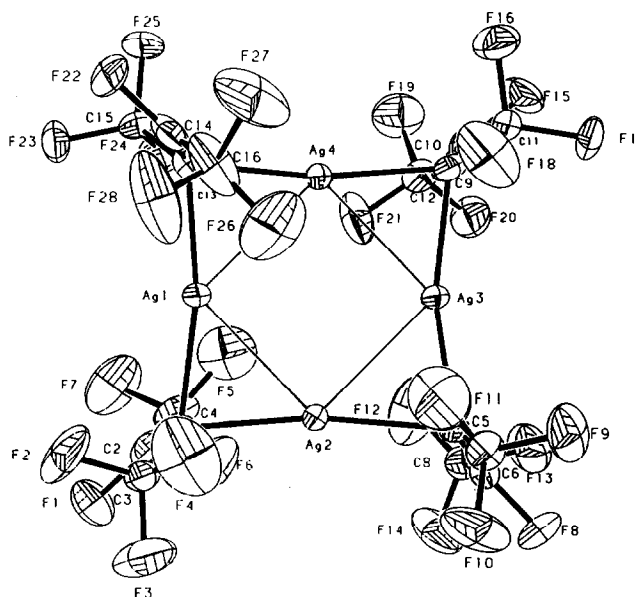


Fig. 1. ORTEP diagram of  $\text{trans-}[\text{CF}_3\text{CF}=\text{C}(\text{CF}_3)\text{Ag}]_4$  (**1**) viewed from above the plane of the silver atoms. Thermal ellipsoids are drawn at the 25% probability level.

noting that the square-planar structure of **1** is similar to those of some  $d^{10}$  copper(I) species such as the alkyl  $[\text{Cu}(\text{CH}_2\text{-SiMe}_3)]_4$ , the alkoxide  $[\text{Cu}(\text{O-}^i\text{Bu})]_4$ , and the amide  $[\text{Cu}(\text{NET}_2)]_4$  [21–23].

Figure 2 shows a view of **1** in the plane of the silver atoms. The carbon atoms bonded to the silver atoms lie slightly out of the plane of the silver atoms (C1, 0.23 Å; C5, -0.67 Å; C9, 0.12 Å; and C13, -0.20 Å). All of the perfluoro-1-methyl-1-propenyl ligands are oriented roughly perpendicularly to the plane of the silver atoms. Somewhat surprisingly, the  $\alpha$ -trifluoromethyl groups of *three* of the ligands are located above this plane, while the  $\alpha$ -trifluoromethyl group of the remaining ligand is located below the plane of the silver atoms. Crystal packing forces are probably responsible for this arrangement of the ligands, since there should be no

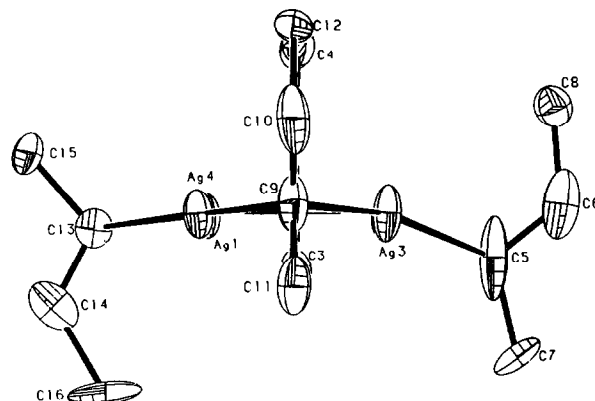


Fig. 2. ORTEP diagram of  $\text{trans-}[\text{CF}_3\text{CF}=\text{C}(\text{CF}_3)\text{Ag}]_4$  (**1**) viewed in the plane of the silver atoms. Thermal ellipsoids are drawn at the 25% probability level. The fluorine atoms have been deleted for clarity. The rear ligand is hidden behind the front ligand.

electronic preference for this structure and on steric grounds one would expect the isolated molecule to have two of the perfluoro-1-methyl-1-propenyl ligands oriented in one direction and two in the other.

## 2.2. MOCVD studies

Sublimation of **1** and passage of the resulting gas at 275°C and  $10^{-4}$  Torr over borosilicate glass substrates yields mirror-like deposits of silver that are 0.5 to 2.0  $\mu\text{m}$  in thickness. The deposits can be removed from the substrates in the form of sheets up to  $4 \times 4$  mm in size. X-ray photoelectron spectroscopy confirms the presence of silver and indicates the presence of small amounts (< 1%) of fluorine and oxygen and the absence of carbon (Fig. 3). Depth profile studies suggest that the oxygen detected probably results from air oxidation of the deposits after they are removed from the MOCVD apparatus, since the amount of oxygen present decreases with increasing depth. Scanning electron micrographs reveal that the films are not

TABLE 3. Selected bond distances (Å) and angles (deg) for  $[\text{CF}_3\text{CF}=\text{C}(\text{CF}_3)\text{Ag}]_4$  (**1**)

Bond Distances	Ag(1)–Ag(2)	2.751(1)	Ag(2)–Ag(3)	2.755(1)	
	Ag(3)–Ag(4)	2.759(1)	Ag(1)–Ag(4)	2.778(1)	
	Ag(1)–C(1)	2.16(1)	Ag(1)–C(13)	2.16(1)	
	Ag(2)–C(1)	2.19(1)	Ag(2)–C(5)	2.27(1)	
	Ag(3)–C(5)	2.20(1)	Ag(3)–C(9)	2.17(1)	
	Ag(4)–C(9)	2.18(1)	Ag(4)–C(13)	2.16(1)	
	Bond Angles	Ag(1)–Ag(2)–Ag(3)	89.92(4)	Ag(2)–Ag(3)–Ag(4)	90.56(4)
		Ag(1)–Ag(4)–Ag(3)	89.28(4)	Ag(2)–Ag(1)–Ag(4)	90.24(4)
C(1)–Ag(1)–C(13)		169.2(5)	C(1)–Ag(2)–C(5)	166.0(5)	
C(5)–Ag(3)–C(9)		161.2(6)	C(9)–Ag(4)–C(13)	170.2(5)	
Ag(1)–C(1)–Ag(2)		78.5(4)	Ag(2)–C(5)–Ag(3)	76.1(5)	
Ag(3)–C(9)–Ag(4)		78.5(5)	Ag(1)–C(13)–Ag(4)	80.1(4)	

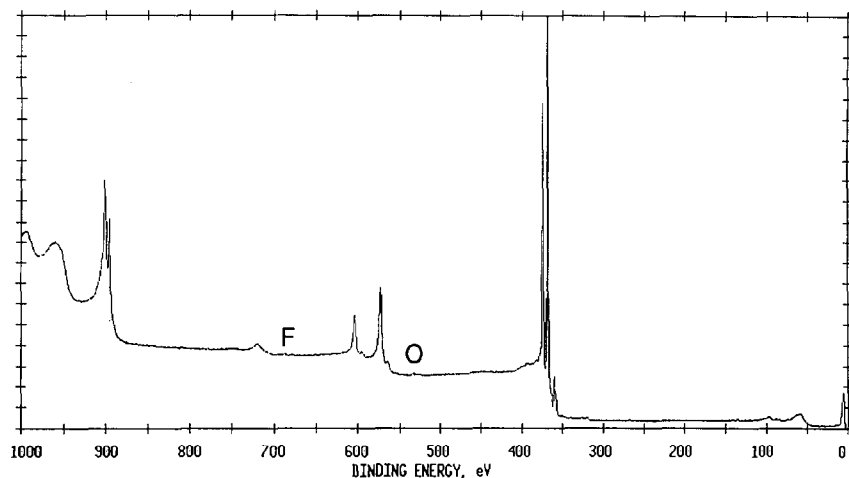


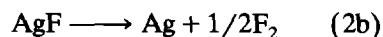
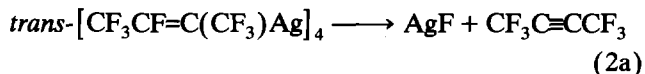
Fig. 3. X-ray photoelectron spectrum of a silver film on borosilicate glass obtained by MOCVD from *trans*- $[CF_3CF=C(CF_3)Ag]_4$  (**1**) at 275°C. All peaks are from silver except those noted.

uniform, but consist of agglomerations of particles with some voids apparent (Fig. 4). The films do not diffract X-rays coherently and are evidently amorphous.

Using a static vacuum apparatus, the byproduct gases formed during the deposition have been collected and analyzed by  $^{19}F$  and  $^1H$  NMR spectroscopy. The principal compounds detected are *trans*- $CF_3CF=CH(CF_3)$  (50%) and  $CF_3C\equiv CCF_3$  (40%); small amounts of other unidentified products are also formed. The peak assignments were confirmed by comparisons with reported chemical shifts and coupling constants for *trans*- $CF_3CF=CH(CF_3)$  [24,25] and  $CF_3C\equiv CCF_3$  [26]. The chemical shifts and coupling constants for *cis*-

$CF_3CF=CH(CF_3)$  [24] have been reported and no peaks in the spectrum can be attributed to this species.

Several steps are necessary to account for the products observed when silver is deposited from **1**. Silver metal is probably formed in two steps: elimination of  $AgF$  from **1** followed by defluorination of  $AgF$ :



The first step would account for the presence of  $CF_3C\equiv CCF_3$  among the reaction products. In fact, this step is the reverse of the reaction by which **1** is synthesized; solution decomposition studies of **1** in sealed NMR tubes show that this elimination reaction occurs readily at 100°C in several hours. The expected defluorination product,  $F_2$ , is however not detected among the deposition byproducts by NMR spectroscopy probably because it reacts further (see below).

The defluorination of bulk  $AgF$  to silver metal at atmospheric pressure has been shown to occur at temperatures as low as 270°C [27]. The thermal stability of  $AgF$  is known to be greatly affected by the experimental conditions [27], and the rate of defluorination from the bulk phase is probably limited by bulk diffusion of fluorine atoms to the surface, where they can dissociate. Since bulk diffusion is not necessary in a MOCVD process, which is inherently a surface phenomenon, the rate of defluorination of  $AgF$  under MOCVD conditions should be at least as fast as the rate of defluorination from the bulk phase.

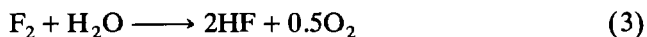
The other organic product formed during deposition of  $Ag$  from **1**, *trans*- $CF_3CF=CH(CF_3)$ , could be produced in several ways. First,  $Ag-C$  bond cleavage could



Fig. 4. Scanning electron micrograph at 15 kV showing the morphology of the silver film obtained by MOCVD from *trans*- $[CF_3CF=C(CF_3)Ag]_4$  (**1**) at 275°C.

occur to form a CF<sub>3</sub>CF=C·(CF<sub>3</sub>) radical which could then abstract a proton from the glass walls of the apparatus to yield *trans*-CF<sub>3</sub>CF=CH(CF<sub>3</sub>). However, decomposition studies of perhydroalkenyl silver compounds indicate that these compounds do *not* decompose via free radical mechanisms [28]. A second possibility is that adventitious water or surface hydroxyl species on the glass walls could effect the hydrolysis of **1** of CF<sub>3</sub>CF=CH(CF<sub>3</sub>) and silver(I) oxide; a similar hydrolysis reaction in solution has previously been reported [14]. Furthermore, silver(I) oxide can lose oxygen at temperatures as low as 240°C to yield silver metal [27]. Despite the ability of this reaction sequence to explain the presence of both the organic and inorganic products observed, related MOCVD studies suggest [29] that there is not sufficient water in the hot zone to account for the amount of *trans*-CF<sub>3</sub>CF=CH(CF<sub>3</sub>) formed.

A third possibility is that CF<sub>3</sub>C≡CCF<sub>3</sub>, produced by elimination of AgF from **1**, reacts with HF produced by eqn. (3) [30] to form *trans*-CF<sub>3</sub>CF=CH(CF<sub>3</sub>) (eqn. (4)).



Although relatively little water is present as a gas phase species in the hot zone, the formation of HF by eqn. (3) could occur by direct reaction of F<sub>2</sub> with the glass walls [30] or more likely at the end of the deposition run when the contents of the liquid-nitrogen-cooled NMR tube warm to room temperature. Equations (2)–(4) are attractive as a reaction sequence because only one decomposition pathway for **1** is required to explain the presence of both CF<sub>3</sub>C≡CCF<sub>3</sub> and *trans*-CF<sub>3</sub>CF=CH(CF<sub>3</sub>) among the organic products.

If eqns. (2)–(4) describe the actual reaction sequence, then the addition of HF to CF<sub>3</sub>C≡CCF<sub>3</sub> must occur specifically to give the observed *trans* alkene. The addition of HX to dialkylacetylenes generally yields *trans* alkenes [31]; furthermore, it is known that *trans*-CF<sub>3</sub>CF=CH(CF<sub>3</sub>) is thermodynamically more stable than the *cis* isomer; heating a mixture of the two isomers in the presence of a fluoride catalyst gives the *trans* isomer only (> 95%) [24,32]. It has also been proposed that the formation of the *cis* isomer is kinetically disfavored due to the steric repulsions between the trifluoromethyl groups. It therefore seems likely that the addition of HF to CF<sub>3</sub>C≡CCF<sub>3</sub> could occur specifically to give the *trans* isomer.

The key feature of this proposed reaction sequence is that the ultimate product, silver metal, is formed via an intermediate phase, silver(I) fluoride. This proposed mechanism is similar to that by which copper metal is

deposited from the copper(I) alkoxide complex [Cu(O-<sup>t</sup>Bu)]<sub>4</sub>; elimination of isobutylene and tert-butanol gives copper(I) oxide, Cu<sub>2</sub>O, which in a second step deoxygenates to give copper metal [29]. This CVD process and that responsible for the deposition of silver metal from **1** are made possible by the relative ease of reduction of Cu<sup>I</sup> to Cu<sup>0</sup> and of Ag<sup>I</sup> to Ag<sup>0</sup>; in the former case the reduction is a deoxygenation reaction, while in the latter case the reduction is a defluorination reaction. Under the low-pressure conditions under which these depositions are conducted, both reductions are thermodynamically favored.

### 2.3. Concluding remarks

The volatile silver complex *trans*-perfluoro-1-methyl-1-propenylsilver has been examined crystallographically, and has been shown to adopt a tetrameric square-planar structure in the solid state, in which the silver centers have approximately linear two-coordinate geometries and the perfluoro-1-methyl-1-propenyl ligands bridge the square edges. This complex is the first to serve as a precursor for the chemical vapor deposition of silver films, not only under plasma assisted conditions [13], but also under thermal CVD conditions. The organic byproducts generated during the deposition process have been identified as *trans*-CF<sub>3</sub>CF=CH(CF<sub>3</sub>) and CF<sub>3</sub>C≡CCF<sub>3</sub>. The formation of silver metal from *trans*-[CF<sub>3</sub>CF=C(CF<sub>3</sub>)Ag]<sub>4</sub> is proposed to occur via elimination of CF<sub>3</sub>C≡CCF<sub>3</sub> to form AgF, which subsequently defluorinates under CVD conditions to generate silver metal. This CVD process, like that responsible for the deposition of copper metal from [Cu(O-<sup>t</sup>Bu)]<sub>4</sub>, emphasizes that the deposition of thin films from metal-organic precursors is often a multistep process that may involve intermediate phases that are unstable under CVD conditions.

### 3. Experimental section

All operations were carried out under vacuum or argon. Acetonitrile and methylene chloride were distilled under nitrogen from calcium hydride before use. Silver(I) fluoride (Cerac) and hexafluoro-2-butyne (PCR) were used without further purification.

Elemental analyses were carried out by Mr. Thomas McCarthy of the School of Chemical Sciences Micro-analytical Laboratory at the University of Illinois. Infrared spectra were recorded on a Perkin-Elmer 599B instrument as Nujol mulls between KBr plates. The <sup>1</sup>H and <sup>19</sup>F NMR data were recorded on a Varian Unity 400 spectrometer at 400 and 376 MHz, respectively. Chemical shifts are reported in δ units (positive chemical shifts to high frequency) relative to SiMe<sub>4</sub> (<sup>1</sup>H) or CCl<sub>4</sub> (<sup>19</sup>F). Hexafluorobenzene was used as a chemi-

cal shift reference for the  $^{19}F$  NMR experiments. X-ray photoelectron spectra were induced by a 15 kV, 400 W Mg  $K\alpha$  radiation source (1253.6 eV) on a Perkin-Elmer 5400 ESCA/Auger system with a pass energy of 89.45 eV and an energy resolution of 0.5 eV/step. The samples were argon sputtered to remove surface contamination before spectra were obtained. Scanning electron micrographs were obtained on an ISI DS-130 instrument.

### 3.1. *trans*-Perfluoro-1-methyl-1-propenylsilver (1)

This compound was prepared by modification of a published procedure [14]. At all times, **1** was handled in the dark or under red light. A Fisher-Porter bottle was loaded with silver(I) fluoride (1.26 g, 0.01 mol) and a stir bar. The bottle was evacuated and pressurized to 15 psi with hexafluoro-2-butyne (0.02 mol). The amount of hexafluoro-2-butyne used was determined by weighing the gas cylinder before and after addition. The Fisher-Porter bottle was then cooled to  $-78^\circ C$  to condense the 1,1,1,4,4,4-hexafluoro-2-butyne, and acetonitrile (20 ml) was added to the bottle. The resulting mixture was stirred at room temperature for three days to yield a clear solution and some black precipitate. The solution was transferred from the Fisher-Porter bottle into a separate flask, and the solvent was removed under vacuum. The product was sublimed from the residue at  $110^\circ C$  and  $10^{-3}$  Torr. The product was further purified by recrystallization from methylene chloride, and was identified by comparison of its IR spectrum with the spectrum reported in the literature [14]. Yield: 1.2 g (42%). Anal. Calcd: C, 16.3; H, 0. Found: C, 15.1; H, 0.4%. (The carbon analysis is low presumably due to incomplete combustion, a situation often characteristic of fluorocarbons. The error in the hydrogen analysis is comparable to the amount found. Water is not present in the product as shown by IR spectroscopy.)  $^{19}F$  NMR ( $C_6D_6$ ,  $25^\circ C$ ):  $\delta$  - 49.5 ( $J_{FF} = 16$  Hz,  $\alpha$ - $CF_3$ ), -57.3 (br s, CF), -68.8 (d,  $J_{FF} = 13$  Hz,  $\beta$ - $CF_3$ ). IR ( $cm^{-1}$ ): 1675sh, 1634m, 1560w, 1509w, 1453m, 1311s, 1244s, 1192s, 1122s, 1088s, 1021sh, 960w, 893m, 850m, 800w, 735m, 693w, 650m, 612w, 573m, 537w, 510w.

### 3.2. Chemical vapor deposition of silver from *trans*-perfluoro-1-methyl-1-propenylsilver (1)

The hot wall, dynamic vacuum apparatus has been described in detail elsewhere [33]. The precursor reservoir was maintained at  $110^\circ C$ , the deposition temperature was  $275^\circ C$ , and the deposition pressure was  $10^{-4}$  Torr. The deposition took place over a 12 h period; less than 10% of the precursor decomposes in the reservoir over this period.

### 3.3. Static vacuum chemical vapor deposition studies and analysis of gaseous byproducts

The static vacuum apparatus and procedure used has been described in detail elsewhere [29]. The deposition was conducted at  $275^\circ C$  under a static vacuum initially at  $10^{-4}$  Torr. The liberated volatile products were condensed into an NMR tube as they were formed. At the end of the deposition run, benzene- $d_6$  was condensed into the NMR tube, which was then flame sealed. The byproducts of the deposition run were analyzed by  $^1H$  and  $^{19}F$  NMR spectroscopy. NMR data for  $CF_3C\equiv CCF_3$ :  $^{19}F$  NMR ( $C_6D_6$ ,  $25^\circ C$ ):  $\delta$  - 53.1 (s). NMR data for *trans*- $CF_3CF=CHCF_3$ :  $^1H$  NMR ( $C_6D_6$ ,  $25^\circ C$ ): 85.99 (dq,  $^3J_{FF} = 29$  Hz,  $^3J_{HF} = 7$  Hz).  $^{19}F$  NMR ( $C_6D_6$ ,  $25^\circ C$ ):  $\delta$  - 59.3 (ddq,  $^3J_{HF} = 7$  Hz,  $^4J_{FF} = 17$  Hz,  $^5J_{FF} = 1.5$  Hz,  $CHCF_3$ ), -73.8 (dq,  $^3J_{FF} = 10$  Hz,  $^5J_{FF} = 1.5$  Hz,  $CFCF_3$ ), -118.0 (ddq,  $^3J_{HF} = 29$  Hz,  $^4J_{FF} = 17$  Hz,  $^3J_{FF} = 10$  Hz,  $CFCF_3$ ).

### 3.4. Crystallographic studies

Single crystals of  $[CF_3CF=C(CF_3)Ag]_4$  (**1**), grown from methylene chloride, were mounted on glass fibers with Paratone-N oil (Exxon) and immediately cooled to  $-75^\circ C$  in a nitrogen stream on the diffractometer. The sample was protected from exposure to light. Standard peak search and indexing procedures gave preliminary unit cell parameters, and the diffraction symmetry was confirmed by inspection of axial photographs. Least-squares refinement of 25 reflections gave the final unit cell parameters listed in Table 1 [34].

Data were collected in one quadrant of reciprocal space ( $+h$ ,  $+k$ ,  $\pm l$ ) by using the measurement parameters listed in Table 1. Systematic absences for  $0k0$ ,  $k \neq 2n$  and  $h0l$ ,  $l \neq 2n$  were consistent with space group  $P2_1/c$ . The measured intensities were reduced to structure factor amplitudes and their esd's by correction for background, scan speed, Lorentz, and polarization effects. While corrections for crystal decay were unnecessary, absorption corrections were applied, the maximum and minimum factors being 0.492 and 0.415, respectively. Systematically absent reflections were deleted and symmetry equivalent reflections were averaged to yield the set of unique data. Only those data with  $I > 2.58\sigma(I)$  were used in the least squares refinement.

The structure was solved using direct methods (SHELXS-86). The correct positions for the silver atoms were deduced from an E-map. Subsequent least-squares refinement and difference Fourier calculations revealed the position of the remaining atoms. Independent refinement of F and C atomic positions converged with C-C and C-F bond lengths that were less than 0.9 Å. All attempts to refine a disordered model were unsuccessful. Atomic positions were therefore refined

using bond length constraints preceding each least-squares cycle: C–F<sub>o</sub>,  $1.33 \pm 0.01$  Å; C=C,  $1.33 \pm 0.01$  Å; C–C,  $1.51 \pm 0.01$  Å. The quantity minimized by the least-squares program was  $\sum w(|F_o| - |F_c|)^2$ , where  $w = 5.18/(\sigma(F_o)^2 + (pF_o)^2)$ . The analytical approximations to the scattering factors were used, and all structure factors were corrected for both the real and imaginary components of anomalous dispersion. In the final cycle of least squares, all atoms were refined with anisotropic thermal coefficients. Successful convergence was indicated by the maximum shift/error of 0.003 for the last cycle. The highest peaks in the final difference Fourier map were in the vicinity of the silver atoms. A final analysis of variance between observed and calculated structure factors showed a slight dependence on  $\sin \theta$ . Tables of anisotropic thermal parameters, complete bond distances and angles, and a table of final observed and calculated structure factors are available from G.S.G. and will be deposited in the Cambridge Crystallographic Data Base.

#### Acknowledgments

We thank the Department of Energy (Contract DE-AC 02-76 ER 1198) and the National Science Foundation (DMR 88-09854) through the Science and Technology Center for Superconductivity for funding. XPS and XPD were carried out in the Center for Microanalysis of Materials, University of Illinois, which is supported by the US Department of Energy under contract DE-AC 02-76ER 01198. SEM was performed at the Center for Electron Microscopy at the University of Illinois. We particularly thank Teresa Prussak-Wieckowska of the University of Illinois X-ray Crystallographic Laboratory for assistance with the crystallographic studies. P.M.J. is the recipient of a University of Illinois Department of Chemistry Fellowship. G.S.G. acknowledges an A.P. Sloan Foundation Research Fellowship and a Henry and Camille Dreyfus Teacher-Scholar Award (1988–1993).

#### References

- 1 Y. Matsumoto, J. Hombo and Y. Yamaguchi, *Mater. Res. Bull.*, **24** (1989) 1231.
- 2 S. Y. Lee, T. S. Han, Y. H. Kim and S. S. Choi, *J. Appl. Phys.*, **68** (1990) 856.
- 3 J. H. Choy, D. Y. Jung, J. C. Grenier, J. C. Park and A. Wattiaux, *Mater. Lett.*, **10** (1990) 121.
- 4 G. Kozłowski, S. Rele, D. F. Lee and K. Salama, *J. Mater. Sci.*, **26** (1991) 1056.

- 5 D. Marsh, F. Arammash, J. Bennett, R. Deck, A. R. El Ali, D. E. Weeks and A. M. Hermann, *Appl. Phys. Commun.*, **9** (1989-90) 245.
- 6 K. H. Song, H. K. Liu, S. X. Dou, C. C. Sorrell, N. Savvides and G. J. Bowden, *J. Mater. Sci.: Mater. Elec.*, **1** (1990) 30.
- 7 C. J. Kim, M. S. Hahn, D. S. Suhr, K. B. Kim, H. J. Lee, H. G. Lee, G. W. Hong and D. Y. Won, *Mater. Lett.*, **11** (1991) 79.
- 8 J. M. Zhang, B. W. Wessels, L. M. Tonge and T. J. Marks, *Appl. Phys. Lett.*, **56** (1990) 976.
- 9 R. Singh, S. Sinha, N. J. Hsu and P. Chou, *J. Appl. Phys.*, **67** (1990) 1562.
- 10 K. Zhang, E. P. Boyd, B. S. Kwak, A. C. Wright and A. Erbil, *Appl. Phys. Lett.*, **55** (1989) 1258.
- 11 J. M. Zhang, H. O. Marcy, L. M. Tonge, B. W. Wessels, T. J. Marks and C. R. Kannewurf, *Appl. Phys. Lett.*, **55** (1989) 1906.
- 12 G. Van Koten and J. G. Noltes, in G. Wilkinson (ed.), *Comprehensive Organometallic Chemistry*, Oxford, 1982; Vol. 2, Chapter 14.
- 13 C. Oehr and H. Suhr, *Appl. Phys. A.*, **49** (1989) 691.
- 14 W. T. Miller, R. H. Snider and R. J. Hummel, *J. Am. Chem. Soc.*, **91** (1969) 6532.
- 15 C. D. M. Beverwijk, G. J. M. Van Der Kerk, A. J. Leusink and J. G. Noltes, *Organomet. Chem. Rev. A.*, **5** (1970) 215.
- 16 A. N. Nesmeyanov, N. N. Sedova, Y. T. Struchkov, V. G. Andrianov, E. N. Stakheeva and V. A. Sazonova, *J. Organomet. Chem.*, **153** (1987) 115.
- 17 M. E. Meyer, S. Gambarotta, C. Floriani, A. Chiesi-Villa and C. Guastini, *Organometallics*, **8** (1989) 1067.
- 18 R. R. Burch and J. C. Calabrese, *J. Am. Chem. Soc.*, **108** (1986) 5359.
- 19 J. Emsley, *The Elements*, Clarendon, Oxford, 1989; p. 174.
- 20 P. K. Mehrotra and R. Hoffmann, *Inorg. Chem.*, **17** (1978) 2187.
- 21 J. A. J. Jarvis, R. Pearce and M. F. Lappert, *J. Chem. Soc., Dalton Trans.*, (1977) 999.
- 22 T. Greiser and E. Weiss, *Chem. Ber.*, **109** (1976) 3142.
- 23 H. Hope and P. P. Power, *Inorg. Chem.*, **23** (1984) 936.
- 24 R. D. Chambers and A. J. Palmer, *Tetrahedron*, **25** (1969) 4217.
- 25 W. R. Cullen and D. S. Dawson, *Can. J. Chem.*, **45** (1967) 2887.
- 26 C. H. Duncan and J. R. Van Wazer, *Compilation of Reported F<sup>19</sup> NMR Chemical Shifts*, Wiley Interscience, New York, 1970.
- 27 T. Flóra and I. Gaál, *Thermochim. Acta*, **7** (1973) 173.
- 28 G. M. Whitesides, C. P. Casey and J. K. Krieger, *J. Am. Chem. Soc.*, **93** (1971) 1379.
- 29 P. M. Jeffries, L. H. Dubois and G. S. Girolami, *Chem. Mater.*, **4** (1992) 1169.
- 30 T. A. O'Donnell, in J. C. Bailar, H. J. Emeléus, R. S. Nyholm and A. F. Trotman-Dickenson (eds.), *Comprehensive Inorganic Chemistry*, Pergamon, Oxford, 1973; Vol. 2, Chapter 25.
- 31 F. A. Carey and R. J. Sundberg, *Advanced Organic Chemistry, Part A: Structure and Mechanisms*, 2nd ed.; Plenum, New York, 1984; p. 342.
- 32 R. D. Chambers, S. Partington and D. B. Speight, *J. Chem. Soc., Perkin Trans. 1*, (1974) 2673.
- 33 G. S. Girolami, J. A. Jensen, J. E. Gozum and D. M. Pollina, *Mat. Res. Soc. Symp. Proc.*, **121** (1988) 429.
- 34 For details of the data collection and refinement procedures see: J. A. Jensen, S. R. Wilson and G. S. Girolami, *J. Am. Chem. Soc.*, **110** (1988) 4977.